Ultraviolet dynamics from ground-state overlap in the Kondo model

C. D. Pelwan and I. Snyman*

Mandelstam Institute for Theoretical Physics, School of Physics, University of the Witwatersrand, P.O. Box Wits, Johannesburg, South Africa

(Received 10 December 2018; revised manuscript received 4 February 2019; published 22 February 2019)

We consider a quantum quench from the strongly correlated ground state of the Kondo model to a Fermi sea. We calculate the overlap between the ground states before and after the quench, as well as the Loschmidt echo, i.e., the transition amplitude between the initial state and the evolved state at a time t after the quench. The overlap is known to determine the dynamics of the echo at large times. We show, in addition, that the overlap depends algebraically on the emergent Kondo length, with a power-law exponent that is the difference of long and short-time contributions that appear in the echo. Our result suggests that, in general, there may be more information contained in the overlap than previously recognized.

DOI: 10.1103/PhysRevB.99.075432

I. INTRODUCTION

When a many-body Hamiltonian is suddenly quenched, the system's full response cannot always be calculated perturbatively. A quantity that captures this singularity is the overlap between the ground states before and after the quench. Due to its fundamental role in nonequilibrium dynamics [1] and quantum phase transitions [2], ground-state–to–ground-state overlaps have been calculated in settings ranging from quantum impurity models [3–5] through single-particle and many-body localized systems [6–8], to spin chains [9,10] and lattices [11], Luttinger liquids [12], and particles with fractional exclusion statistics [13] using techniques that include conformal field theory, the numerical renormalization group, matrix product states, and tensor networks.

Since the overlap compares ground states, it is not surprising that it provides information about infrared (IR) physics, such as long-time dynamics. For instance, if the interaction between a Fermi liquid and a local impurity is suddenly quenched, the transition amplitude between the initial ground state and the time-evolved state after the quench—the Loschmidt echo—decays algebraically at long times, with an exponent equal to that governing the system size dependence of the overlap [1,14–18]. However, unlike truly infrared probes, the ground-state–to–ground-state overlap is determined by the whole Fermi sea, not just the Fermi surface [4]. It must therefore also contain information about properties beyond the infrared. We believe that this aspect of the overlap has been neglected because of a too-narrow focus on the overlap's dependence on the system size—an infrared scale. To remedy this oversight, we study a model with an emergent scale and consider the overlap's dependence on this scale. We are not the first to do so [4,5], but the additional ingredient in our study is the link we establish to nonequilibrium dynamics beyond the infrared.

The rest of this paper is structured as follows. First we define the anisotropic Kondo model that we study and state our main results. Then we present our analysis, which is based on the coherent-state expansion—a representation of the Kondo ground state in terms of a discrete set of bosonic coherent states—that is, in principle, exact. Next we present our (numerical) results and then end the main text with a paragraph summarizing our conclusions. Seven Appendixes contain further background, technical details, and additional numerical results.

II. MODEL AND MAIN RESULTS

We consider a one-dimensional Fermi sea, coupled to a spin-1/2 magnetic moment via a local exchange interaction $J_\parallel S_z(0)s_z + J_\perp[S_x(0)s_x + S_y(0)s_y]$. Here $\vec{S}(0)$ is the electron spin density at $x = 0$, and $\vec{s}$ is the impurity spin. The interaction famously generates an emergent scale, the Kondo temperature T_k. The impurity spin and the Fermi sea form a spin singlet in which the impurity is screened by the electron gas at distances larger than the Kondo length $\xi = \hbar v_F/2T_k$, where v_F is the Fermi velocity. Below we set $\hbar = v_F = 1$. We consider quenches $(J_\parallel, J_\perp) \to (J'_\parallel, 0)$. The vanishing transverse coupling $J'_\perp = 0$ in the final Hamiltonian produces a diverging Kondo length $\xi' \to \infty$. This is associated with imperfect screening of the impurity spin, and the initial and final Hamiltonians therefore have distinct infrared properties. Quenches in the Kondo and related models have been studied numerous times before, both theoretically [17–27] and experimentally [28], but the connection between the ground-state–to–ground-state overlap and dynamics beyond the infrared has not.

Using a combination of analytical and numerical techniques, we calculated the Loschmidt echo $P(t) = \langle J_\parallel, J_\perp | e^{-iH_{J'_\parallel,0}t} | J_\parallel, J_\perp \rangle$, where $|J_\parallel, J_\perp\rangle$ is the ground state before and $H_{J'_\parallel,0}$ the Hamiltonian after the quench. We found distinct power laws in the regimes $t \ll \xi$ and $t \gg \xi$, i.e.,

$$|P(t)| \propto \begin{cases} \left(\frac{a}{t}\right)^{\chi/2} & \text{if } a \ll t \ll \xi, \\ \left(\frac{a}{\xi}\right)^{\chi/2}\left(\frac{\xi}{t}\right)^{\beta/2} & \text{if } \xi \ll t \ll L, \end{cases} \tag{1}$$

*izaksnyman1@gmail.com

where L is the system size, and a is a short-distance cutoff of the order of the Fermi wavelength. The exponent β that governs the IR dynamics ($t \gg \xi$) equals the exponent that appears in the Anderson orthogonality theorem, in agreement with previous studies [1,4], and depends on $J'_\parallel$ but not on the parameters of the prequench Hamiltonian, provided $J_\perp$ is finite. In contrast, the UV exponent depends on both $J_\parallel$ and $J'_\parallel$. Next we calculated the ground-state–to–ground-state overlap $Q \equiv |\langle J_\parallel, J_\perp | J'_\parallel, 0\rangle|^2$ and found

$$Q = C(J_\parallel, J'_\parallel)\left(\frac{a}{\xi}\right)^{\chi/2}\left(\frac{\xi}{L}\right)^{\beta/2}. \tag{2}$$

As is known already [1,3], the L dependence of the overlap is governed by the same exponent that governs the IR dynamics of the echo. In contrast, the overlap's ξ dependence at fixed $J_\parallel$ reveals a new power law with an exponent equal to the difference between the UV and IR exponents of the echo. This is our main result.

Previous studies [4,5] considered the quench $(J_\parallel, J_\perp) \to (J_\parallel, J'_\perp)$, i.e., $J_\parallel$ was held fixed during the quench, and in general the Kondo length was quenched between finite values ξ and ξ'. A very nontrivial analytical result was obtained for the case of a finite postquench Kondo length. However, in the limit $\xi' \gg \xi$, i.e., quenching to $J'_\perp = 0$, this result reduces to the simple power law $|\langle J_\parallel, J_\perp | J'_\parallel, J'_\perp\rangle|^2 \propto (\xi/\xi')^{\beta/2}$ reminiscent of the overlap between Fermi seas, with ξ' playing the role of system size and ξ that of Fermi wavelength. The $(\xi/t)^{\beta/2}$ factor in our result for $P(t)$ is consistent with this interpretation: it coincides with the IR response of a Fermi sea with Fermi wavelength ξ. In [4,5], no ultraviolet contribution to the power-law exponent for ξ was found. Consistent with this, we find that up to finite-size errors, the ultraviolet contribution χ in Eq. (2) vanishes when we choose $J_\parallel = J'_\parallel$. For the overlap to be sensitive to ultraviolet physics, it is therefore essential to have $J_\parallel \neq J'_\parallel$. It is tempting to interpret the factor $(a/\xi)^{\chi/2}$ in Eq. (2) and the factor $(a/t)^{\chi/2}$ in Eq. (1) in terms of Anderson's orthogonality theorem and conclude that the physics above the Kondo scale also allows an effective description in terms of (phase-shifted) Fermi seas. In the UV effective theory, ξ would play the role of an effective system size. For sufficiently large $J_\parallel$, we can show analytically that this picture is indeed correct. In this regime the exponent χ approximately equals the power-law exponent one would obtain by applying the Anderson orthogonality theorem to the trivial initial state obtained by setting $J_\perp = 0$ in the prequench Hamiltonian. However, for smaller $J_\parallel$, the analytical argument breaks down and we find numerically that χ starts to deviate from the $J_\perp \to 0$ result. In the absence of analytical results, we cannot prove conclusively that a UV Fermi sea picture is correct, but if it is, there is a renormalization of $J_\parallel$ from its bare value.

III. ANALYSIS

In our analysis, we exploit the exact mapping known to exist between the Kondo model with nonuniversal ultraviolet scales integrated out and the Ohmic spin-boson model [29–31]. Given a microscopic Kondo Hamiltonian that accounts for physics at all length scales down to the lattice constant, one integrates out UV modes far from the Fermi energy but stops the mode elimination at a scale $1/a$ well above the Kondo temperature. At energy scales below this cutoff, the microscopic model is equivalent to an effective Hamiltonian,

$$H = \sum_{n\in Z;\sigma=\uparrow,\downarrow} q_n c^\dagger_{n\sigma} c_{n\sigma} + \frac{\tilde{J}_\parallel}{2}\sigma_z[\psi^\dagger_\uparrow\psi_\uparrow - \psi^\dagger_\downarrow\psi_\downarrow] + \tilde{J}_\perp[\sigma_-\psi^\dagger_\uparrow\psi_\downarrow + \sigma_+\psi^\dagger_\downarrow\psi_\uparrow], \tag{3}$$

involving linearly dispersing electrons $c_{n\sigma}$, with $q_n = 2\pi n/L$, $n \in Z$, in a single (unfolded) chiral channel. Here $\sigma_\pm = \sigma_x \pm i\sigma_y$ and σ_j, $j = x, y, z$ are Pauli matrices acting on the impurity spin. The operator

$$\psi_\sigma = \sum_n e^{-a|q_n|/2} c_{n\sigma} \tag{4}$$

creates an electron in a wave packet centered around the origin and with group velocity v_F. The width of the wave packet is $\sim a$, and this enforces a soft UV cutoff at the scale at which mode elimination was halted. The Kondo couplings renormalize to $\tilde{J}_\parallel$ and $\tilde{J}_\perp$. Using the fact that mode elimination leaves physics at energies below $1/a$ unchanged and that Kondo physics only sets in at $T_k \ll 1/a$, it is possible to calibrate $\tilde{J}_\parallel$ with respect to the original microscopic model. This gives $\tilde{J}_\parallel = 2\varphi$, where φ is the difference in phase shifts between spin-up and spin-down electrons at the Fermi energy, when instead of the exchange interaction, the bare Fermi sea is subjected to a spin-dependent static potential $J_\parallel S_z(0)$. The value of $\tilde{J}_\perp$ depends on system-specific ultraviolet details in a way that is hard to calculate in practice. However, many infrared properties of the system, among them the ones we consider, are universal functions of the Kondo scale, and this allows one to make nontrivial statements about the behavior of the system without knowledge of the relation between the microscopic parameters and the renormalized $\tilde{J}_\perp$.

The spin-boson model describes a two-level system linearly coupled to a bath of harmonic oscillators. The Hamiltonian is

$$H_{\alpha,\Delta} = \sum_{n=1}^{\infty}\omega_n b^\dagger_n b_n - \sqrt{\alpha}\sum_{n=1}^{\infty}\frac{g_n}{2}(b_n + b^\dagger_n)\sigma_z + \frac{\Delta}{2}\sigma_x, \tag{5}$$

where b_n are bosonic annihilation operators. We take $\Delta > 0$ and denote the ground state of $H_{\alpha,\Delta}$ as $|\alpha, \Delta\rangle$. In the thermodynamic limit, the bath spectrum becomes dense, and the bath is completely characterized by the spectral function $J(\omega) = \sum_{n=1}^{\infty} g_n^2\delta(\omega - \omega_n)$. Typically, a spectral function with an infrared power law is considered. Below, we derive some results assuming a spectral density of the general form

$$J(\omega) = 2\omega_0^{1-s}\omega^s e^{-a\omega}, \tag{6}$$

where $e^{-a\omega}$ is a soft UV cutoff. Using operator bosonization, the low-energy Hamiltonian (3) can be mapped onto $H_{\alpha,\Delta}$ with

$$\omega_n = [\hbar v_F]q_n, \quad g_n = 2\sqrt{\frac{\pi q_n}{L}}e^{-aq/2}, \tag{7}$$

and

$$\alpha = \left(\frac{\tilde{J}_\parallel}{2\pi} - 1\right)^2 = \left(\frac{\varphi}{\pi} - 1\right)^2, \quad \Delta = \frac{\tilde{J}_\perp}{\pi a}. \tag{8}$$

In the thermodynamic limit, the resulting spectral density is of the form (6) with $s = 1$, i.e., a linear spectral density at low frequency. This is referred to as the Ohmic case.

In the thermodynamic limit, one introduces Dirac-δ normalized bosonic field operators $\phi_\omega = \lim_{L\to\infty} \sqrt{L/2\pi} b_n$ and calculates the Kondo length as follows [32]:

$$\xi = \lim_{\omega\to 0} \langle \alpha, \Delta | \frac{\phi_\omega + \phi_\omega^\dagger}{\sqrt{2\omega}} \sigma_z | \alpha, \Delta \rangle. \tag{9}$$

In the fermionic language the above definition translates to $\xi = \lim_{x\to\infty} 4x^2 \langle S_z(x) s_z \rangle$. The familiar Kondo temperature, defined via the static spin susceptibility [33], is related to the Kondo length [34] as $T_K = 1/2\xi$. For the Kondo quenches we are interested in, we must evaluate the spin-boson Loschmidt echo,

$$P(t) = e^{itE_{\alpha',0}} \langle \alpha, \Delta | e^{-iH_{\alpha',0}t} | \alpha, \Delta \rangle, \tag{10}$$

where $E_{\alpha',0}$ is the ground-state energy of $H_{\alpha',0}$. Here, $\alpha' = (\varphi'/\pi - 1)^2$, and the relationship between φ' and $J'_\parallel$ is the same as that between φ and $J_\parallel$.

Our analysis is based on an exact expansion of the ground state of $H_{\alpha,\Delta}$ in terms of a *discrete* set of coherent states. The theory behind the expansion was first set out in Refs. [32,35,36]. Here and in Appendix A, we give a brief review. According to an elementary theorem by Cahill [37], an arbitrary state $|\psi\rangle$ of a set of bosonic modes can be written as a *discrete* sum $|\psi\rangle = \sum_{m=1}^\infty c_m |f_m\rangle$, where $|f_m\rangle$ is a multimode coherent state, i.e., $b_n |f_m\rangle = f_{mn} |f_m\rangle$. The representation is not unique, and there is always sufficient freedom to choose the coefficients f_{mn} real. The spin-boson Hamiltonian is invariant with respect to the unitary transformation T that sends $b_n \to -b_n$ and $\sigma_z \to -\sigma_z$. We confine our attention to the so-called delocalized phase, where the ground state $|\alpha, \Delta\rangle$ transforms under T as $T|\alpha, \Delta\rangle = -|\alpha, \Delta\rangle$, so that $\langle \sigma_z \rangle = 0$. For the Ohmic case ($s = 1$), the interval $\alpha \in (0, 1)$ is within the delocalized phase [38]. With the help of Cahill's theorem, we can then exactly parametrize the ground state as

$$|\alpha, \Delta\rangle = \sum_{m=1}^\infty \frac{c_m}{\sqrt{2}} (|f_m\rangle|\uparrow\rangle - |-f_m\rangle|\downarrow\rangle). \tag{11}$$

In order to put this result to practical use, the sum in Eq. (11) is truncated to a finite number of M terms and the optimal parameters c_m and f_{mn} are found via the variational principle. Any desired accuracy can in principle be attained by taking M sufficiently large. In the limit of small α, the single term expansion $M = 1$ becomes exact [36,39,40]. Significant headway can be made analytically with the minimization (as we review in Appendix A), and as a result, one is eventually left with only $M^2 + M - 1$ parameters whose values must be found via numerical minimization. However, some analytical results can be obtained without explicitly calculating the optimal values of these parameters. An example is a result that we derive in Appendix B, namely, that at large times

$$P(t) \simeq |\langle \alpha, \Delta | \alpha', 0 \rangle|^2 \exp \frac{\alpha'}{4} \int_0^\infty d\omega \frac{J(\omega)}{\omega^2} e^{-i\omega t}. \tag{12}$$

Whereas $P(t)$ is regular in the thermodynamic limit, if the individual factors on the right of Eq. (12) are calculated separately, the calculations must be performed for a finite system size. The time dependence of Eq. (12) is the same as $\exp(iE_{\alpha',0}t)\langle \mathrm{IR}| \exp(-iH_{\alpha',0}t)|\mathrm{IR}\rangle$, with $|\mathrm{IR}\rangle = |0\rangle(|\uparrow\rangle - |\downarrow\rangle)/\sqrt{2}$. This is because in the delocalized phase, the coherent-state parameters f_{mn} tend to zero for modes n whose frequencies ω_n tend to zero [34]. As a result, infrared probes cannot distinguish the initial state from the bosonic vacuum. Specializing now to the Ohmic case, we find that at large times compared to ξ,

$$P(t) = Q\left(\frac{2\pi i t}{L}\right)^{-\beta/2}, \tag{13}$$

with $\beta = \alpha'$ and where we use the Kondo and spin-boson notations $Q \equiv |\langle \alpha, \Delta | \alpha', 0 \rangle|^2$ interchangeably. Since $P(t)$ should not vanish when we take the limit $L \to \infty$, we conclude that $Q \propto L^{-\beta/2}$. In Appendix C we comment further on these known results and explain how they relate to the Anderson orthogonality theorem. In Appendix D we derive an expression for the echo in terms of the variational parameters of the coherent-state expansion that are valid for all times and form the basis of our numerical study below.

Now we turn to the Kondo length dependence of the overlap. We first present a heuristic argument by means of which the numerical results we subsequently present may be anticipated. Provided $\xi \gg a$, we expect ξ to set the scale for dynamics at times sufficiently larger than a. This motivates the scaling ansatz

$$P(t) = Z(\alpha, \alpha', \xi/a) F_{\alpha,\alpha'}\left(\frac{t}{\xi(\alpha, \Delta, a)}\right), \tag{14}$$

in which all parameter dependencies have been rendered explicit. If this ansatz is correct, we can extract Z from the long-time result (13) and obtain

$$Z = \left(\frac{2\pi\xi}{L}\right)^{-\beta/2} Q. \tag{15}$$

Now, consider the behavior of $P(t)$ at times short compared to ξ. We expect the degrees of freedom that are relevant in this regime to be ignorant of physics at the Kondo scale. For large $J_\parallel$, i.e., small α, we can show analytically using the $M = 1$ expansion that for $a \ll t \ll \xi$,

$$P(t) = C\left(\frac{it}{a}\right)^{-\chi/2}, \tag{16}$$

with $\chi = (\varphi/\pi - \varphi'/\pi)^2 = (\sqrt{\alpha} - \sqrt{\alpha'})^2/2$ and C independent of ξ. (See Appendix E for a derivation.) This is the same behavior as we would have obtained if before the quench we had $J_\perp = 0$, and hence $\xi = \infty$. Our analytical argument, however, breaks down at larger α. Let us nonetheless assume that a short-time power law of the form (16) holds for arbitrary α with a ξ-independent C. Universal scaling according to the ansatz (14) implies that $P(t)/Z$ depends only on t and ξ in the

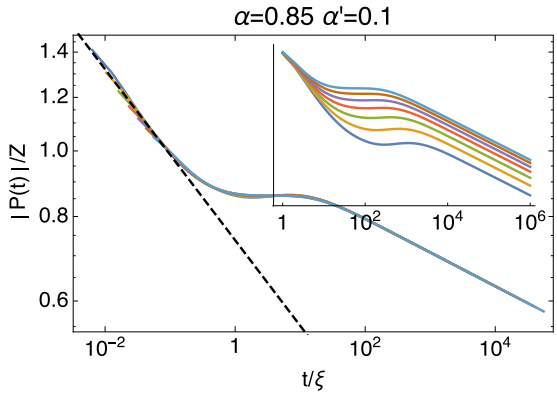

FIG. 1. The computed Loschmidt echo $P(t)$ for $\alpha = 0.85$ and $\alpha' = 0.1$. The different curves correspond different Δ/a values $\in \{0.156, 0.18, 0.205, 0.23, 0.255, 0.28, 0.305\}$. The main panel shows the amplitude of the scaled function $P(t)/Z$ vs t/ξ, with Z and ξ calculated from Eqs. (9) and (15), not fitted. The inset shows the unscaled data vs time in units of a. The sloped dashed line represents the short-time power law (16), with C and χ obtained by fitting to the amplitude data for $t < 10^{-1}\xi$.

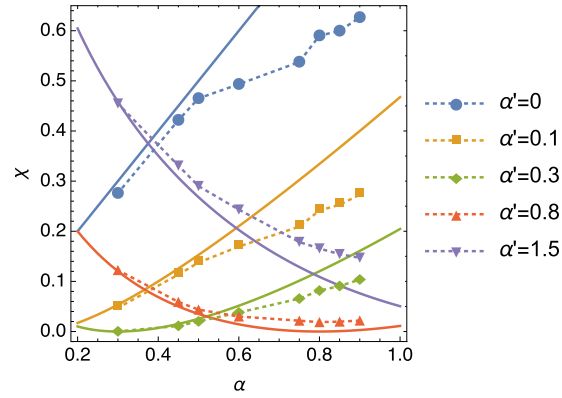

FIG. 2. Symbols: The short-time power-law exponent χ defined in Eq. (16), at five different values of α', as extracted from our numerical $P(t)$ data, an example of which is shown in Fig. 1. Curves: The small α prediction $\chi = (\varphi/\pi - \varphi'/\pi)^2$.

combination t/ξ. The ξ independence of C then implies that $Z \propto \xi^{-\chi/2}$. Using our analytic expression (15) for Z, we arrive at the result we want, namely, $Q \propto \xi^{(\beta-\chi)/2}$. Below Eq. (13) we concluded that the overlap Q scales with system size as $L^{-\beta/2}$. Since the only other length scale that Q can depend on is a, we reproduce Eq. (2), our main result.

IV. RESULTS

In the remainder of this work, we present our numerical study based on the coherent-state expansion. We note that a powerful extension of the technique has been developed to deal with general time-dependent problems [41,42]. However, due to the simple form of the postquench Hamiltonian, no sophisticated techniques are needed here, once the initial state is expressed in terms of the bosons. We reuse the numerical ground-state data of [32]. The data were obtained by simulated annealing for an expansion truncated to $M = 7$ terms at most. In [32], multiple checks were done to verify that numerical convergence is satisfactory. In Appendix F we show how the curves for $P(t)$ calculated at increasing M rapidly converge. We estimate that the error in $P(t)$ is at most on the order of 1% at large times and less at shorter times. For given α, we have data for ξ/a ranging over between 1 and 2 decades, with the shortest ξ an order of magnitude larger than the short-distance cutoff a. For each of the 50 combinations of (α, Δ) at which data was taken, we calculated the Loschmidt echo and the scaling factor Z for quenches to various $\alpha' \in [0, 1.5]$. Further details are provided in Appendix G. In Fig. 1, we show results for the quench $\alpha = 0.85 \to \alpha' = 0.1$ as a representative example. $|P(t)|$ follows a short-time power law in the time window $a < t < \xi$. From the inset we see that $|P(t)|$ is relatively independent of Δ at small t. We see excellent universal scaling in accordance with the ansatz (14). Note that the scaling factors ξ and Z were not determined by fitting, as is frequently done when one looks for universality, but were calculated using Eqs. (9) and (15).

In Fig. 2 we show examples of the short-time power-law exponent we extracted from the Loschmidt echo. For $\alpha \lesssim 0.5$, we find good agreement with the approximate analytical result $\chi = (\varphi/\pi - \varphi'/\pi)^2/2$. At larger α, $|P(t)|$ still obeys a short-time power law, but the power-law exponent deviates from $(\varphi/\pi - \varphi'/\pi)^2/2$. At small α, modes with $1/\xi \ll \omega_n \ll 1/a$ are associated with displacements $f_{mn} \simeq \sqrt{\alpha} g_n/2\omega_n$, as if $\Delta = 0$, and this allows for a straightforward explanation of the power law in terms of the response of noninteracting spin-up and spin-down Fermi seas to a local quench. However, at larger α, we find numerically that the same asymptotic behavior of f_{mn} only sets in close to the ultraviolet cutoff $1/a$. If a noninteracting Fermi sea explanation is possible in this regime, the coherent-state expansion does not make this manifest. When $\alpha = \alpha'$, the analytical result of Refs. [4,5] is that $\chi = 0$. The largest deviation we found from this is $\chi = 0.018$ at $\alpha = \alpha' = 0.8$. We believe this is a small finite-size error, and note that we unambiguously find that χ is minimal when $\alpha = \alpha'$. We also note oscillatory behavior that might be a numerical error in the results for $\alpha' = 0$, 0.1 and $\alpha > 0.6$. The same fluctuations are not seen at other α' values. Given that the same ground-state data was used for

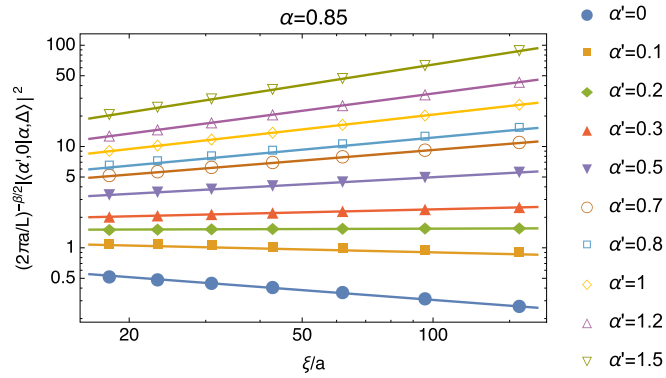

FIG. 3. Symbols: The ground-state–to–ground-state overlap squared $|\langle\alpha', 0|\alpha, \Delta\rangle|^2$ vs the Kondo length ξ for various α', at $\alpha = 0.85$. Lines: The power law $|\langle\alpha', 0|\alpha, \Delta\rangle|^2 = G\xi^\eta$, with G and η obtained by fitting to the data with $\xi \gtrsim 25a$.

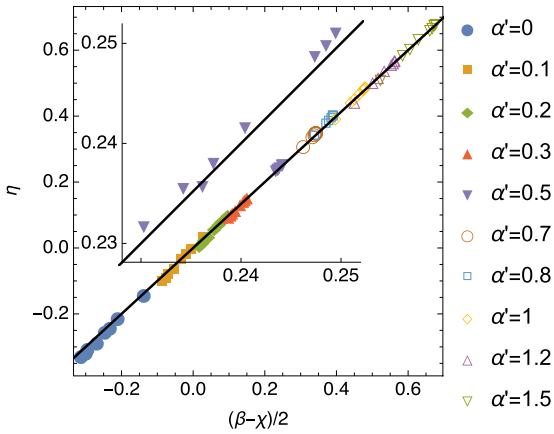

FIG. 4. Symbols: Each data point corresponds to a fixed value of α and β. The x and y coordinates of each point are respectively $(\beta-\chi)/2$, with the short-time power-law exponent χ corresponding to the symbols in Fig. 2, and the power-law exponent η cf. Eq. (17), as extracted from the data in such as that plotted in Fig. 3. Black line: The heuristic prediction $\eta=(\beta-\chi)/2$. Inset: An enlarged view of the clustered $\beta=0.5$ data.

all α', we attribute any error that is present to the numerical extraction of the power-law exponent rather than to errors in the ground-state data.

With the assumption verified that in the regime $a \ll t \ll \xi$ the Loschmidt echo is both independent of Δ and obeys a power law $t^{-\chi/2}$, our conclusion regarding the power-law dependence of the ground-state overlap on the Kondo length must be correct. We have calculated $(2\pi a/L)^{-\beta/2}|\langle\alpha',0|\alpha,\Delta\rangle|^2$ directly and indeed find that at fixed α and α' (i.e., fixed $J_\parallel$ and $J'_\parallel$ in the Kondo language) $|\langle\alpha',0|\alpha,\Delta\rangle|^2=Q$ has a power-law dependence on ξ, i.e.,

$$|\langle\alpha',0|\alpha,\Delta\rangle|^2 \propto \xi^{\eta}. \tag{17}$$

As an example, in Fig. 3, we show results for $\alpha=0.85$ and various α'. In Fig. 4 we compare the power-law exponent η of the overlap, extracted from data such as that shown in Fig. 3, to the short-time power-law exponent χ of the Loschmidt echo, extracted from data such as that shown in Fig. 1. We see very good agreement with our prediction that $\eta=(\beta-\chi)/2$. The largest deviations are seen at $\alpha'=0$, $\alpha>0.6$. As we noted already, the extracted values of the exponent χ for these data points may contain some noise. However, even here, the largest deviation between the extracted η values and the line representing $\eta=(\beta-\chi)/2$ is 5%. For the other data sets, the deviation is of the order of a percent at most.

V. CONCLUSION

For the Kondo model, we have demonstrated that the Loschmidt echo and the overlap between ground states before and after the quench are connected not only via dynamics at long times, but also via dynamics at short times. Our main results are contained in Eqs. (1) and (2) and can be summarized as follows. If one subtracts the slope seen at short times in the log-log plot of the Loschmidt echo (Fig. 1), from the slope seen at long times, one obtains the slope seen in the log-log plot of the ground-state–to–ground-state overlap squared versus the Kondo length (Fig. 3). The overlap's dependence on the emergent length scale ξ thus elegantly encodes information about both IR and UV dynamics. Apart from Anderson's orthogonality theorem, the other essential ingredients that produced this result were the universal scaling and power-law behavior of the Loschmidt echo at short times. In light of this, it may be interesting to revisit results for the overlap in studies of other systems that have focused on system size dependence to see if similar connections exist.

ACKNOWLEDGMENTS

We wish to thank Serge Florens for insightful discussions and comments. This work is based on research supported by the National Research Foundation of South Africa (Grant No. 90657) and the CNRS PICS contract "FermiCats."

APPENDIX A: IDENTIFYING THE VARIATIONAL PARAMETERS OF THE MULTICOHERENT-STATE EXPANSION

As mentioned in the main text, significant headway can be made analytically with the variational optimization of the truncated trial state

$$|\psi\rangle=\sum_{m=1}^{M}\frac{c_m}{\sqrt{2}}(|f_m\rangle|\uparrow\rangle-|-f_m\rangle|\downarrow\rangle). \tag{A1}$$

Here we briefly review the relevant results.

By setting the variation of $\langle H_{\alpha,\Delta}\rangle$ with respect to f_{mn}, $m=\{1,2,\ldots,M\}$ equal to zero, one obtains a set of equations of the form

$$(U\omega_n+V)\begin{pmatrix}f_{1n}\\ \vdots\\ f_{Mn}\end{pmatrix}=\sqrt{\alpha}g_nW, \tag{A2}$$

with ω_n the frequency and g_n the hybridization of the bosonic mode n, as in the spin-boson Hamiltonian (5), and the entries of the real $M\times M$ matrices U and V and the real column vector W depend on the trial state $|\psi\rangle$ but are independent of the mode index n, i.e., the same U, V, and W enter the equations for each n. (See [32] for explicit expressions.) This structure comes about because (a) $H_{\alpha,\Delta}$ is quadratic in b_n and $b_n^\dagger$, and (b) there are no direct processes in $H_{\alpha,\Delta}$ that scatter bosons from a mode n to a mode $n'\neq n$. By noting that each matrix element of the inverse of $U\omega_n+V$ is the ratio of polynomials in w_n that are respectively of order $M-1$ and M, and that the denominator is the same for all elements (being the determinant of $U\omega_n+V$), we discover that

$$f_{m,n}=\frac{\sqrt{\alpha}g_n}{2}h_m(\omega_n),\quad h_m(z)=\frac{\sum_{l=0}^{M-1}\mu_{m,l}z^l}{\prod_{l=1}^{M}(z-\Omega_l)}, \tag{A3}$$

where $\mu_{m,l}$ is real. Furthermore, because $U\omega_n+V$ is real, the Ω_l that are not real come in complex conjugate pairs. It is intuitively clear that for modes with natural frequencies $\omega_n\gg\Delta$, the tunneling term $\Delta\sigma_x/2$ becomes a negligible perturbation and hence, i.e., $f_{mn}\simeq\sqrt{\alpha}g_n/2\omega_n$. This implies that $\mu_{m,M-1}=1$. The same conclusion follows rigorously from the observation that associated with mode n, there are

unavoidable positive contributions to the energy proportional to $\omega_n(f_{mn} - \sqrt{\alpha}g_n/2\omega_n)^2$. Energy considerations also dictate that there are no poles Ω_l on the positive real line. Finding the $M^2 + M - 1$ unknown parameters Ω_m, $\mu_{m_1m_2}$, and c_m variationally constitutes a global minimization problem that we solve numerically. However, as we show below, some exact results for quench dynamics can also be derived without explicitly computing the optimal Ω_m, $\mu_{m_1m_2}$, and c_m.

APPENDIX B: LONG-TIME BEHAVIOR OF THE LOSCHMIDT ECHO

Here we give a simple analytical derivation of the long-time behavior of the Loschmidt echo based on the coherent-state expansion. The derivation does not require explicit computation of the optimal values of the variational parameters and is valid for an expansion with an arbitrary number M of terms. We believe the result is therefore exact.

First note that the ground-state energy of the postquench Hamiltonian $H_{\alpha',0}$ is

$$E_0' = -\alpha' \sum_{n=1}^{\infty} \frac{g_n^2}{4\omega_n}. \tag{B1}$$

Next, note that because $H_{\alpha',0}$ preserves the z component of spin and is quadratic in boson operators, it is straightforward to compute the time evolution of $|\alpha, \Delta\rangle$. After some algebra, these observations lead to the result

$$\begin{aligned} P(t) = \sum_{m_1,m_2} c_{m_1} c_{m_2} \langle f_{m_1} | \alpha' + \rangle \langle \alpha' + | f_{m_2} \rangle \\ \times \exp \frac{1}{4} \sum_{n=1}^{\infty} g_n^2 \left[\frac{\sqrt{\alpha'}}{\omega_n} - \sqrt{\alpha} h_{m_1}(\omega_n) \right] \\ \times \left[\frac{\sqrt{\alpha'}}{\omega_n} - \sqrt{\alpha} h_{m_2}(\omega_n) \right] e^{-i\omega_n t}, \end{aligned} \tag{B2}$$

where

$$|\alpha' \pm\rangle = \exp \pm \sqrt{\alpha'} \sum_{n=1}^{\infty} \frac{g_n}{2\omega_n} (b_n^\dagger - b_n) |0\rangle, \tag{B3}$$

so that $|\alpha'+\rangle|\uparrow\rangle$ and $|\alpha'-\rangle|\downarrow\rangle$ are the two degenerate ground states of $H_{\alpha',0}$ and

$$\langle f_m | \alpha' + \rangle = \exp -\frac{1}{8} \sum_{n=1}^{\infty} g_n^2 \left[\frac{\sqrt{\alpha'}}{\omega_n} - \sqrt{\alpha} h_m(\omega_n) \right]^2. \tag{B4}$$

At long times, the frequency sum in Eq. (B2) is dominated by the contribution from small frequencies, where g_n/ω_n dominates over $h_m(\omega_n)$. (Recall that the $h_m(\omega)$ remain finite when $\omega \to 0$.) Thus, asymptotically,

$$P(t) \simeq |\langle \alpha, \Delta | \alpha', 0 \rangle|^2 \exp \frac{\alpha'}{4} \sum_{n=1}^{\infty} \frac{g_n^2}{\omega_n^2} e^{-i\omega_n t} \tag{B5}$$

where

$$|\alpha', 0\rangle = (|\alpha'+\rangle|\uparrow\rangle - |\alpha'-\rangle|\downarrow\rangle)/\sqrt{2} \tag{B6}$$

is the ground state of $H_{\alpha',0}$ with T eigenvalue -1. In the thermodynamic limit it is convenient to rewrite this result as

$$P(t) \simeq |\langle \alpha, \Delta | \alpha', 0 \rangle|^2 \exp \frac{\alpha'}{4} \int_0^{\infty} d\omega \frac{J(\omega)}{\omega^2} e^{-i\omega t} \tag{B7}$$

using the bath spectral function $J(\omega)$.

APPENDIX C: KONDO MODEL AND ANDERSON'S ORTHOGONALITY THEOREM

The algebraic decay $t^{-\alpha'/2}$ and $L^{-\alpha'/2}$ of respectively the Loschmidt echo and the overlap has been obtained before, for instance, using numerical renormalization group technology [3]. It is a manifestation of the fact that under renormalization, the Kondo ground state (of the prequench Hamiltonian) flows to a strong-coupling infrared fixed point of the form $|\mathrm{IR}\rangle = (|\theta = -\pi\rangle|\uparrow\rangle - |\theta = \pi\rangle|\downarrow\rangle)/\sqrt{2}$. Here, we use the notation $|\theta\rangle$ to represent a noninteracting Fermi sea in which electrons undergo phase shifts that depend on their spin direction, such that at the Fermi energy these phase shifts equal $\theta/2$ and $-\theta/2$ for spin-up and spin-down electrons, respectively. The postquench ground state, on the other hand, is of the form $|\varphi', \infty\rangle = (|\theta = -\varphi'\rangle|\uparrow\rangle - |\theta = \varphi'\rangle|\downarrow\rangle)/\sqrt{2}$. The power-law behavior of the overlap can be understood by replacing the true initial state with $|\mathrm{IR}\rangle$ and applying the celebrated Anderson orthogonality theorem, which states that $|\langle \pm\pi | \pm \varphi' \rangle|^2 \propto (L/\lambda_F)^{-(1/2-\varphi'/2\pi)^2}$, where λ_F is the Fermi wavelength and the proportionality constant is of order unity. Since the infrared fixed point of the Kondo model is reached when length scales shorter than $\sim \xi$ are integrated out, the effective Fermi wavelength to use when applying the Anderson orthogonality theorem is of order ξ. Another classic result in many-body theory [16] states that for noninteracting fermions, the Loschmidt echo decays algebraically $\propto (\varepsilon_F t)^{-(1/2-\varphi'/2\pi)^2}$, with the same power-law exponent as that governing the L dependence of the overlap. When applying this result to the long-time dynamics of the Kondo model, the effective Fermi energy to use is $\varepsilon \sim \hbar v_F/\xi$. Finally, we note that the coherent-state expansion provides an analytic derivation of these results. The derivation is exact because no restriction is placed on the number M of terms to which the expansion is truncated.

APPENDIX D: FURTHER ANALYTICAL PROGRESS IN THE OHMIC CASE

It is useful to write the Loschmidt echo (B2) as

$$P(t) = \sum_{m_1 m_2} c_{m_1} c_{m_2} \langle f_{m_1} | \alpha' + \rangle \langle \alpha' + | f_{m_2} \rangle P_{m_1 m_2}(t), \tag{D1}$$

where

$$\begin{aligned} P_{m_1 m_2}(t) = \exp \sum_{n=1}^{\infty} \frac{\pi q_n e^{-(a+it)q_n}}{L} \Big\{ \alpha h_{m_1}(q_n) h_{m_1}(q_n) \\ - \frac{\sqrt{\alpha\alpha'}}{q_n} \big[h_{m_1}(q_n) + h_{m_2}(q_n) \big] + \frac{\alpha'}{q_n^2} \Big\}. \end{aligned} \tag{D2}$$

The first and second terms in the curly brackets need no infrared regularization and we can replace the sum over discrete modes with an integral. We cannot do the same with

the third term. Here, however, the discrete sum is computed straightforwardly.

$$\sum_{n=1}^{\infty}\frac{\pi\alpha' e^{-aq_n}}{Lq_n}e^{-(a+it)q_n}=-\frac{\alpha'}{2}\ln[1-e^{-2\pi(a+it)/L}]. \quad \text{(D3)}$$

Thus

$$P_{m_1m_2}(t)=[1-e^{-2\pi(a+it)/L}]^{-\alpha'/2}\times\exp\left\{\frac{\alpha}{2}A_{m_1m_2}(t)-\frac{\sqrt{\alpha\alpha'}}{2}\left[B_{m_1}(t)+B_{m_2}(t)\right]\right\}, \quad \text{(D4)}$$

where

$$A_{m_1m_2}(t)=\int_0^\infty dq\,qe^{-q(a+it)}h_{m_1}(q)h_{m_2}(q),$$
$$B_m(t)=\int_0^\infty dq\,e^{-q(a+it)}h_m(q). \quad \text{(D5)}$$

Also,

$$\langle\alpha'+|f_m\rangle=\exp\left[-\frac{\alpha}{4}A_{mm}(0)+\frac{\sqrt{\alpha\alpha'}}{2}B_m(0)\right]\left(\frac{2\pi a}{L}\right)^{\alpha'/4}. \quad \text{(D6)}$$

The fact that $h_m(q)$ is a rational function of q allows us to perform the above integrals analytically. Using a method explained in detail in [32], we obtain

$$\begin{aligned}A_{m_1m_2}(t)&=e^{-i\phi}\sum_{l=1}^{M}\mathrm{Res}\left[qe^{-i\phi}h_{m_1}(qe^{-i\phi})h_{m_2}(qe^{-i\phi})\times F(q|a+it|),q=\Omega_l e^{i\phi}\right]\\&=\sum_{l=1}^{M}\left\{\left[h_{m_1l}h_{m_2l}+\Omega_l\left(\dot{h}_{m_1l}h_{m_2l}+h_{m_1l}\dot{h}_{m_2l}\right)\right]\times F[\Omega_l(a+it)]-\Omega_l(a+it)h_{m_1l}h_{m_2l}\times\left[F[\Omega_l(a+it)]+\frac{1}{\Omega_l(a+it)}\right]\right\} \quad \text{(D7)}\end{aligned}$$

and

$$B_m(t)=e^{-i\phi}\sum_{l=1}^{M}\mathrm{Res}\left[h_{m_1}F(q|a+it|),q=\Omega_l e^{i\phi}\right]=\sum_{l=1}^{M}h_{m_1l}F[\Omega_l(a+it)], \quad \text{(D8)}$$

where $F(z)=e^{-z}\Gamma(0,-z)$ and $\Gamma(\gamma,z)$ is the incomplete Γ function. The phase ϕ is the argument of $a+it$, i.e., $e^{i\phi}=(a+it)/|a+it|$, while

$$h_{ml}=\lim_{q\to\Omega_l}(q-\Omega_l)h_m(q)=\frac{\sum_{n=0}^{M-1}\mu_{mn}\Omega_l^n}{\prod_{n=1\neq l}^{M}(\Omega_l-\Omega_n)}, \quad \text{(D9)}$$

and

$$\dot{h}_{ml}=\lim_{q\to\Omega_l}\frac{d}{dq}[(q-\Omega_l)h_m(q)]=\frac{\sum_{n=1}^{M-1}\mu_{mn}n\Omega_l^{n-1}}{\prod_{n=1\neq l}^{M}(\Omega_l-\Omega_n)}-h_{ml}\sum_{n=1\neq l}^{M}\frac{1}{\Omega_l-\Omega_n}. \quad \text{(D10)}$$

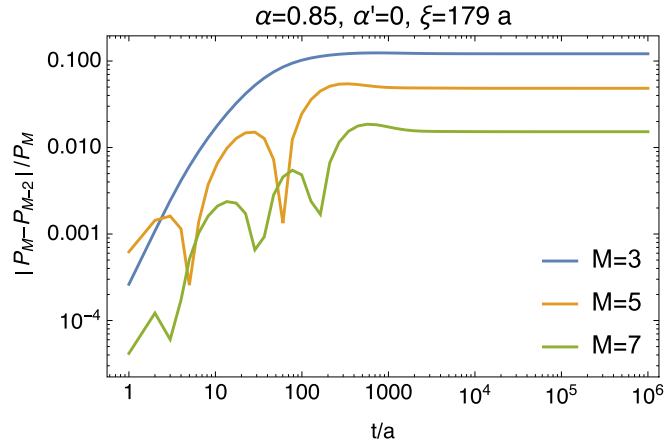

FIG. 5. The relative change in $P(t)$ when the number of terms in the trial state is incremented by 2. Results are shown for $\alpha=0.85$ and $\Delta=0.157a$. We estimate $\xi=180a$. We show curves for $\alpha'=0$.

In these formulas we assume that the poles Ω_l of $h_m(q)$ all have negative real parts, a fact that we have not proven. It is, however, borne out by the numerics. Furthermore, the additional terms that would occur if there were poles with positive real parts would only introduce additional contributions to the Loschmidt echo that decay exponentially over time and are unimportant at large times. These equations form the basis of our numerical study of the full $P(t)$. For future reference, we express the Kondo length ξ and the scaling factor Z, as introduced in the main text, in terms of the ground-state parameters:

$$\xi=\frac{\sqrt{\alpha}}{2}\sum_{m_1m_2}c_{m_1}c_{m_2}\left[h_{m_1}(0)+h_{m_2}(0)\right]\langle f_{m_1}|f_{m_2}\rangle, \quad \text{(D11)}$$

$$Z=\left(\frac{2\pi\xi}{L}\right)^{-\alpha'/2}|\langle\alpha',0|\alpha,\Delta\rangle|^2=\left(\frac{\xi}{a}\right)^{-\alpha'/2}\left|\sum_{m=1}^{M}c_m\exp\left[-\frac{\alpha}{4}A_{mm}(0)+\frac{\sqrt{\alpha\alpha'}}{2}B_m(0)\right]\right|^2. \quad \text{(D12)}$$

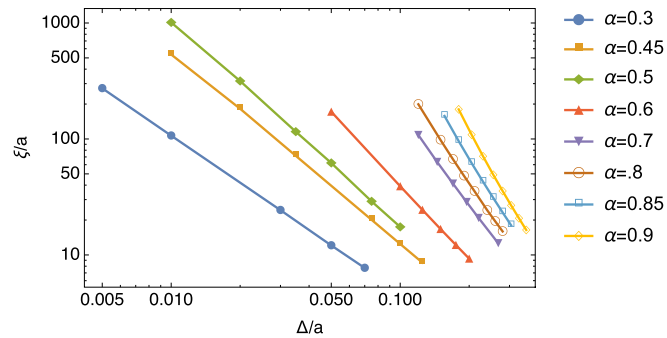

FIG. 6. The calculated Kondo length ξ for each of the parameter values (α,Δ) for which the ground state of $H_{\alpha,\Delta}$ was numerically calculated. Lines connect data points corresponding to the same α.

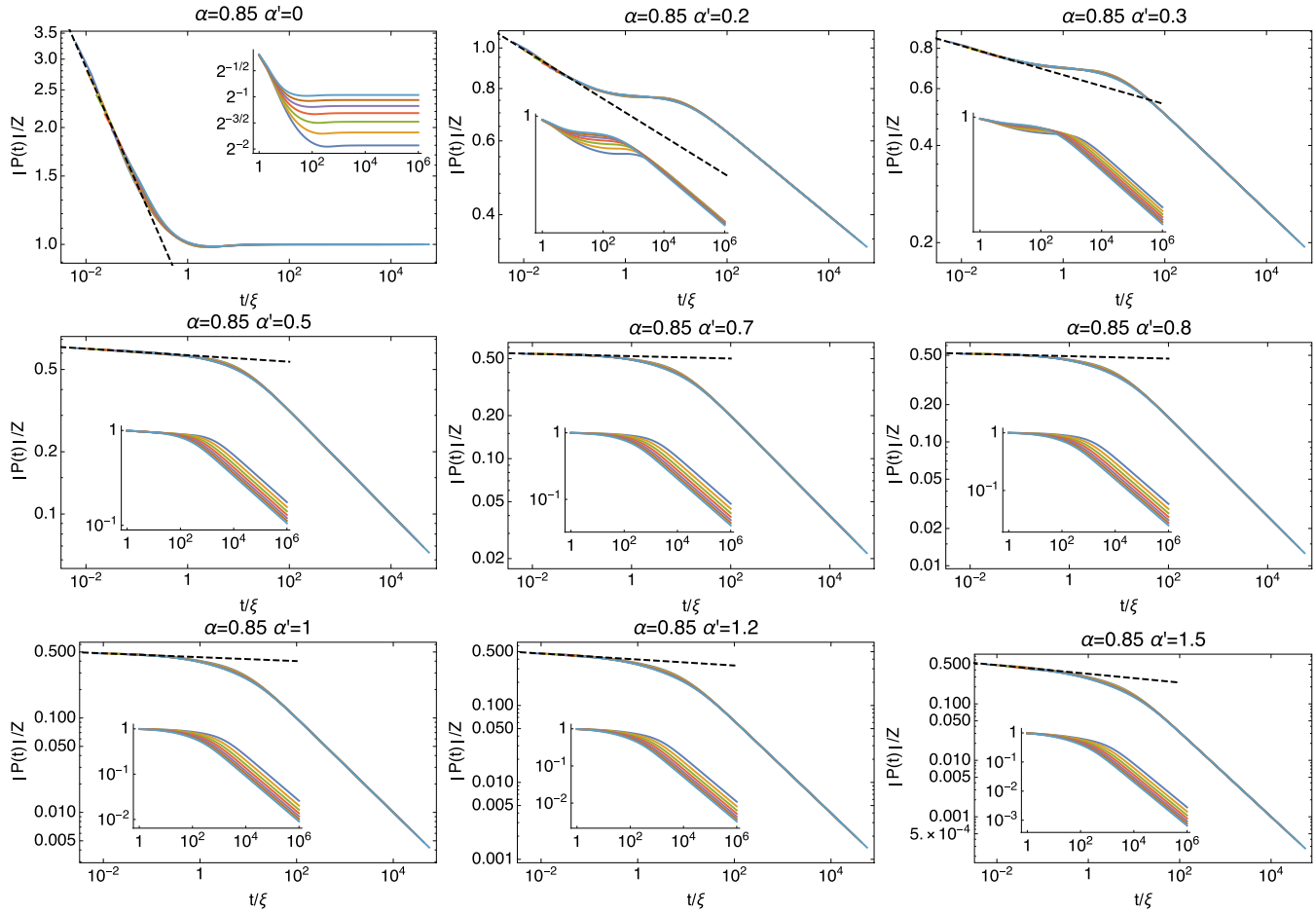

FIG. 7. The amplitude of the computed Loschmidt echo $P(t)$ for $\alpha = 0.85$. Different panels correspond to different α' values. The different curves correspond to different Δ/a values $\in \{0.156, 0.18, 0.205, 0.23, 0.255, 0.28, 0.305\}$. The main panel shows the amplitude of the scaled function $P(t)/Z$ vs t/ξ, with Z and ξ calculated from Eqs. (D11) and (D12). The inset shows the unscaled data vs time in units of a. The sloped dashed line represents the short-time power law $|P| = C(t/a)^{-\xi/2}$, with C and χ obtained by fitting to the amplitude data for $t < 10^{-1}\xi$.

APPENDIX E: ANALYTICAL RESULTS AT SMALL α

The coherent-state expansion truncated to a single term ($M = 1$) is known as the Silbey-Harris ansatz [39,40]. The Silbey-Harris ansatz is exact for small α. Here we use this fact to obtain an explicit expression for $P(t)$ in the limit of small α. We use this expression to give an analytical derivation of the short-time power law of $P(t)$, valid for sufficiently small α. For $M = 1$, there is only one variational parameter Ω_1. Its optimal value is $-\Delta_R$ where Δ_R satisfies

$$\Delta_R = \Delta\langle f_1|-f_1\rangle = \Delta \exp -\alpha A_{11}(0) < \Delta. \tag{E1}$$

The Kondo length is

$$\xi = \frac{\sqrt{\alpha}}{\pi\,\Delta_R}. \tag{E2}$$

For $A_{11}(t)$ and $B_1(t)$ we obtain

$$\begin{aligned} A_{11}(t) &= [1 + \Delta_R(a + it)]F[-\Delta_R(a + it)] - 1 \\ B_1(t) &= F[-\Delta_R(a + it)], \end{aligned} \tag{E3}$$

and for $P(t)$ we obtain

$$P(t) = \left(\frac{it}{a}\right)^{-\alpha'/2} \times \exp\left\{\frac{\alpha}{2}[A_{11}(t) - A_{11}(0)] - \sqrt{\alpha\alpha'}[B_1(t) - B_1(0)]\right\}. \tag{E4}$$

Provided Δ is sufficiently smaller than $1/a$, we have $\Delta_R a$, $\Delta_R t \ll 1$ in the regime $a \ll t <\!\!< \xi$ and we can expand $F[-\Delta_R(a + it)]$ for small arguments using $F(-z) = -\ln(z) - \gamma_E + \mathcal{O}(z)$, where $\gamma_E = 0.57\ldots$ is the Euler-Mascheroni constant. We then find $[A_{11}(t) - A_{11}(0)] = [B_1(t) - B_1(0)] = -\ln(1 + it/a)$ independent of ξ, and

$$P(t) = \left(\frac{it}{a}\right)^{-\chi/2}, \tag{E5}$$

with $\chi = (\sqrt{\alpha} - \sqrt{\alpha'})^2$. We note that the same result would be obtained if we took $f_{1n} = \sqrt{\alpha}g_n/2\omega_n$. In the Kondo language this corresponds to the initial state $|\mathrm{UV}\rangle = (|-\varphi\rangle|\uparrow\rangle - |\varphi\rangle|\downarrow\rangle)/\sqrt{2}$, with $\varphi = \pi(1 - \sqrt{\alpha})$. Here $|\pm\varphi\rangle$ represents a noninteracting Fermi sea in which electrons undergo phase shifts that depend on their spin direction, such

that at the Fermi energy these phase shifts equal $\pm\varphi/2$ and $\mp\varphi/2$ for spin-up and spin-down electrons, respectively.

APPENDIX F: CONVERGENCE OF THE MULTICOHERENT-STATE EXPANSION

In Ref. [32] numerous tests were performed to demonstrate that a sufficient number of terms were included to ensure good convergence of the numerically obtained ground-state data. Here we provide one more piece of evidence. For given α and Δ, we optimize multipolaron trial states with successively larger M. Because of parity effects, we increase M by 2 in each step. We then calculate the relative change in $P(t)$ as M is increased. In Fig. 5, we show the results obtained at the least converged data point in our full data set, namely, $\alpha = 0.85$, $\Delta = 0.157a$. We consider $\alpha' = 0$, which corresponds to the case where the extracted short-time power-law exponent is likely least accurate. We see that convergence is better for smaller t. This is easy to understand: optimizing ultraviolet degrees of freedom is prioritized, because this yields greater energy gains than optimizing infrared degrees of freedom. We also see the rapid convergence of the ansatz: the change in P drops by roughly $\sqrt{10}$ between successive increments of M by 2. We therefore expect the $P(t)$ curve for $M = 7$ to be accurate to about 1%, with a higher accuracy at short times.

APPENDIX G: FURTHER NUMERICAL RESULTS

Here we provide some further numerical results. In Fig. 6 we plot the Kondo lengths associated with each of the ground states we obtained numerically. In Fig. 7 we plot the rest of numerical Loschmidt echo data for the $\alpha = 0.85$ data set. (The data for $\alpha' = 0.1$ was already presented in the main text.)

[1] W. Münder, A. Weichselbaum, M. Goldstein, Y. Gefen, and J. von Delft, Anderson orthogonality in the dynamics after a local quantum quench, Phys. Rev. B **85**, 235104 (2012).

[2] S.-J. Gu, Fidelity approach to quantum phase transitions, Int. J. Mod. Phys. B **24**, 4371 (2010).

[3] A. Weichselbaum, W. Münder, and J. von Delft, Anderson orthogonality and the numerical renormalization group, Phys. Rev. B **84**, 075137 (2011).

[4] S. L. Lukyanov, H. Saleur, J. L. Jacobsen, and R. Vasseur, Exact Overlaps in the Kondo Problem, Phys. Rev. Lett. **114**, 080601 (2015).

[5] S. L. Lukyanov, Fidelities in the spin-boson model, J. Phys. A **49**, 164002 (2016).

[6] V. Khemani, R. Nandkishore, and S. L. Sondhi, Nonlocal adiabatic response of a localized system to local manipulations, Nat. Phys. **11**, 560 (2015).

[7] D.-L. Deng, J. H. Pixley, X. Li, and S. Das Sarma, Exponential orthogonality catastrophe in single-particle and many-body localized systems, Phys. Rev. B **92**, 220201(R) (2015).

[8] R. Vasseur and J. E. Moore, Multifractal orthogonality catastrophe in one-dimensional random quantum critical points, Phys. Rev. B **92**, 054203 (2015).

[9] P. Zanardi and N. Paunković, Ground state overlap and quantum phase transition, Phys. Rev. E **74**, 031123 (2006).

[10] M. Cozzini, R. Ionicioiu, and P. Zanardi, Quantum fidelity and quantum phase transition in matrix product states, Phys. Rev. B **76**, 104420 (2007).

[11] H.-Q. Zhou, R. Orus and G. Vidal, Ground State Fidelity from Tensor Network Representations, Phys. Rev. Lett. **100**, 080601 (2008).

[12] A. O. Gogolin, Local Time-Dependent Perturbation in Luttinger Liquid, Phys. Rev. Lett. **71**, 2995 (1993).

[13] F. Ares, K. S. Gupta, and A. R. de Queiroz, Orthogonality catastrophe and fractional exclusion statistics, Phys. Rev. E **97**, 022133 (2018).

[14] G. Yuval and P. W. Anderson, Exact results for the Kondo problem: One-body theory and extension to finite temperature, Phys. Rev. B **1**, 1522 (1970).

[15] J. J. Hopfield, Infrared divergences, x-ray edges, and all that, Comments Solid State Phys. **2**, 40 (1969).

[16] K. Ohtaka and Y. Tanabe, Theory of the soft-x-ray edge problem in simple metals: Historical survey and recent developments, Rev. Mod. Phys. **62**, 929 (1990).

[17] R. Vasseur, K. Trinh, S. Haas, and H. Saleur, Crossover Physics in the Nonequilibrium Dynamics of Quenched Quantum Impurity Systems, Phys. Rev. Lett. **110**, 240601 (2013).

[18] D. M. Kennes, V. Meden, and R. Vasseur, Universal quench dynamics of interacting quantum impurity systems, Phys. Rev. B **90**, 115101 (2014).

[19] P. Nordlander, M. Pustilnik, Y. Meir, N. S. Wingreen, and D. C. Langreth, How Long Does it Take for the Kondo Effect to Develop? Phys. Rev. Lett. **83**, 808 (1999).

[20] F. B. Anders and A. Schiller, Real-Time Dynamics in Quantum-Impurity Systems: A Time-Dependent Numerical-Renormalization-Group Approach, Phys. Rev. Lett. **95**, 196801 (2005).

[21] D. Lobaskin and S. Kehrein, Crossover from nonequilibrium to equilibrium behavior in the time-dependent Kondo model, Phys. Rev. B **71**, 193303 (2005).

[22] F. B. Anders and A. Schiller, Spin precession and real-time dynamics in the Kondo model: Time-dependent numerical renormalization group study, Phys. Rev. B **74**, 245113 (2006).

[23] M. Heyl and S. Kehrein, Interaction quench dynamics in the Kondo model in the presence of a local magnetic field, J. Phys.: Condens. Matter **22**, 345604 (2010).

[24] M. Medvedyeva, A. Hoffmann, and S. Kehrein, Spatiotemporal buildup of the Kondo screening cloud, Phys. Rev. B **88**, 094306 (2013).

[25] B. Lechtenberg and F. B. Anders, Spatial and temporal propagation of Kondo correlations, Phys. Rev. B **90**, 045117 (2014).

[26] S. Ghosh, P. Ribeiro, and M. Haque, Dynamics of the impurity screening cloud following quantum quenches of the resonant level model, J. Stat. Mech. (2015) P08002.

[27] J. A. Andrade, A. A. Aligia, and P. S. Cornaglia, Many-body dynamics of the decay of excitons of different charges in a quantum dot, Phys. Rev. B **94**, 235109 (2016).

[28] C. Latta *et al.*, Quantum quench of Kondo correlations in optical absorption, Nature (London) **474**, 627 (2011).

[29] F. Guinea, V. Hakim, and A. Muramatsu, Bosonization of a two-level system with dissipation, Phys. Rev. B **32**, 4410 (1985).

[30] G. Kotliar and Q. Si, Toulouse points and non-Fermi-liquid states in the mixed valence regime of the generalized Anderson model, Phys. Rev. B **53**, 12373 (1996).

[31] T. A. Costi and G. Zaránd, Thermodynamics of the dissipative two-state system: A Bethe-ansatz study, Phys. Rev. B **59**, 12398 (1999).

[32] S. Florens and I. Snyman, Universal spatial correlations in the anisotropic Kondo screening cloud: Analytical insights and numerically exact results from a coherent state expansion, Phys. Rev. B. **92**, 195106 (2015).

[33] M. Hanl and A. Weichselbaum, Local susceptibility and Kondo scaling in the presence of finite bandwidth, Phys. Rev. B **89**, 075130 (2014).

[34] Z. Blunden-Codd, S. Bera, B. Bruognolo, N. O. Linden, A. W. Chin, J. vonDelft, A. Nazir, and S. Florens, Anatomy of quantum critical wave functions in dissipative impurity problems, Phys. Rev. B **95**, 085104 (2017).

[35] S. Bera, A. Nazir, A. W. Chin, H. U. Baranger, and S. Florens, Generalized multipolaron expansion for the spin-boson model: Environmental entanglement and the biased two-state system, Phys. Rev. B **90**, 075110 (2014).

[36] S. Bera, S. Florens, H. U. Baranger, N. Roch, A. Nazir, and A. W. Chin, Stabilizing spin coherence through environmental entanglement in strongly dissipative quantum systems, Phys. Rev. B **89**, 121108(R) (2014).

[37] K. E. Cahill, Coherent-state representation of the photon density operator, Phys. Rev. **138**, B1566 (1965).

[38] R. Bulla, H.-H. Tong, and M. Votja, Numerical Renormalization Group for Bosonic Systems and Application to the Sub-Ohmic Spin-Boson Model, Phys. Rev. Lett. **91**, 170601 (2003).

[39] R. Silbey and R. A. Harris, Variational calculation of the dynamics of a two level system interacting with a bath, J. Chem. Phys. **80**, 2615 (1984).

[40] R. A. Harris and R. Silbey, Variational calculation of the tunneling system interacting with a heat bath, II. Dynamics of an asymmetric tunneling system, J. Chem. Phys. **83**, 1069 (1985).

[41] N. Gheeraert, S. Bera, and S. Florens, Spontaneous emission of Schrödinger cats in a waveguide at ultrastrong coupling, New J. Phys. **19**, 023036 (2017).

[42] N. Gheeraert, X. H. H. Zhang, T. Sépulcre, S. Bera, N. Roch, H. U. Baranger, and S. Florens, Particle production in ultrastrong coupling waveguide QED, Phys. Rev. A **98**, 043816 (2018).